COUPLED PIEZOELECTRIC MICROMACHINED ULTRASONIC TRANSDUCERS WITH IMPROVED PULSE-ECHO PERFORMANCE

Qi Wang, Yuri Kusano, and David A. Horsley
University of California, Davis, CA, USA

ABSTRACT

This paper presents a novel piezoelectric micromachined ultrasonic transducer (PMUT) based on mechanical coupling between a center circular resonator and an outer annular membrane. Compared to traditional circular membrane PMUTs, the design has the advantages that (1) it allows the PMUT diameter to be matched to the acoustic wavelength (λ=190μm at 8MHz) to enable high fill-factor arrays and (2) it achieves much higher TX/RX sensitivity due to mechanical amplification of the input piezoelectric force. The measured displacement is a factor of two greater than a conventional PMUT operating at the same frequency. Pulse echo measurements show a 1.9x and 6.5x increase in transmitting and receiving sensitivity at 6MHz and 8MHz when compared to a conventional PMUT array spanning the same area.

INTRODUCTION

Micromachined ultrasonic transducers (MUTs), due to their better acoustic coupling, lower manufacturing cost and lower power consumption compared to conventional bulk ultrasonic transducers, have been developed for many consumer electronic applications such as gesture sensors [1], fingerprint sensors [2] and medical imaging devices [3]. Recently, with the development of piezoelectric thin film deposition technologies, piezoelectric micromachined ultrasonic transducers (PMUT) arrays have been rapidly developed [4]-[5]. Compared to capacitive micromachined ultrasonic transducers (CMUTs), PMUTs have advantages including reduced interface circuit design complexity because no high voltage is required [6] and lower variation in device-to-device impedance because the dielectric layer is solid rather than an air-gap as it is in a CMUT.

When designing arrays of CMUTs or PMUTs, it is desirable to have a unit cell size that is comparable to the acoustic wavelength, λ. For 8 MHz operation, λ=190μm, and the unit cell is typically composed of a 2x2 array of PMUTs, because a single 190 μm circular PMUT would need to be very thick and therefore would have low bandwidth. However, it is difficult to achieve high fill factor with small diameter PMUTs. For this reason, there is a need for new PMUT designs that can replace the conventional PMUT design, breaking the traditional connection between thickness and cell diameter. A ring-shaped PMUT was recently demonstrated [7] to have good pressure output. Here, we present a design that exploits mechanical coupling between a circular membrane and a surrounding annular membrane. Mechanical coupling is well-known in CMUT and PMUT arrays but has previously been associated with degraded performance [8]. In the structure presented here, the coupling results in greater transmit pressure and receive sensitivity than a conventional 2x2 array of the same area.

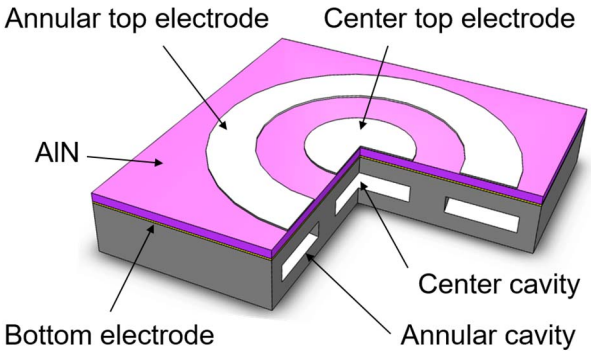

Fig. 1. Coupled PMUT illustration. The cut-away section shows the cavities in the CSOI substrate.

DESIGN AND FABRICATION

Fig. 1 shows an illustration of the proposed coupled PMUT structure, which was fabricated in a cavity SOI (CSOI) process described below. The coupled PMUT consists of a center circular membrane and an outer annular membrane. Two designs of coupled PMUT and conventional circular PMUTs were fabricated on the same wafer to provide a comparison. The dimensions of the two coupled designs and the conventional circular PMUT are listed in Table 1. The PMUTs are composed of 1 μm thick aluminum nitride (AlN) piezoelectric layer, a 200 nm molybdenum (Mo) layer as bottom electrode, a 200 nm aluminum (Al) layer as top electrode and a 2.5 μm thick silicon (Si) membrane.

The resonance frequency in air of the center circular membrane and the outer annular membrane can be calculated from the equation for the undamped resonant frequency with different eigenvalues (λ_{ij}^2),

$$f_{ij} = \frac{\lambda_{ij}^2}{2\pi r^2}\sqrt{\frac{D}{\rho}} \quad (1)$$

where λ_{00}^2 is 10.2 for the circular membrane and 89.2 for the annular membrane, r is the cavity radius of the circular membrane and the outside radius of the outer annular membrane, D is the flexural rigidity and ρ is the average mass per area [8]. Note that λ_{00}^2 for the annular membrane depends on the ratio of the inside and the outside radius.

Table 1, Dimensions of conventional PMUT and coupled PMUT 1 and 2.

Dimension	Conventional PMUT	Coupled PMUT 1	Coupled PMUT 2
Center cavity radius (μm)	30	30	30
Inside radius of annular cavity (μm)	N/A	50	50
Outside radius of annular cavity (μm)	N/A	90	95

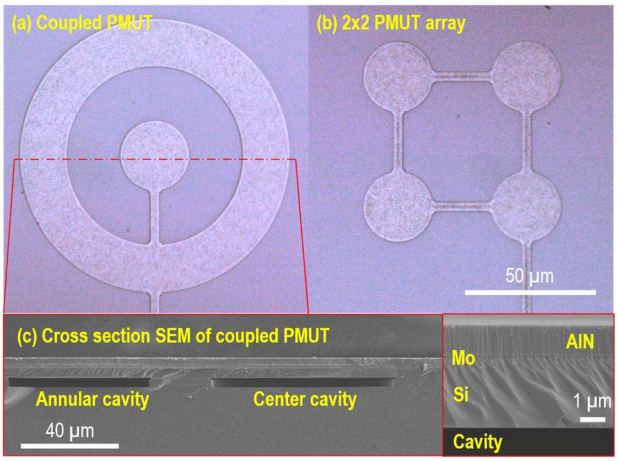

Fig. 2. Optical image of (a) coupled PMUT, (b) conventional 2x2 PMUT array, (c) cross section SEM image of coupled PMUT. The inset shows a close-up of the Mo and AlN layers on top of the 2.5 μm thick Si membrane.

The value of 89.2 provided here applies to a ratio of 0.5. The undamped resonant frequencies of the outer annular membranes of the two coupled PMUT designs were chosen to be either higher (14.0 MHz, PMUT 1) or lower (12.6 MHz, PMUT 2) compared to the center circular membrane's 13.5 MHz undamped resonant frequency. This difference enabled different coupling behaviors to be observed when the PMUTs were immersed in liquid. The resonant frequency of the center circular membrane when immersed can be calculated from equation (2) [8]:

$$f_d = f/\sqrt{1 + 0.67 r \rho_{fluid}/\rho} \qquad (2)$$

where ρ_{fluid} is the density of liquid. Here we used a non-conductive fluid (Fluorinert FC-70, 3M) for immersed measurements. With FC-70, ρ_{fluid} is 1940 kg/m^3, and f_d is 6.25 MHz. The resonant frequencies predicted by these analytical models were confirmed using a finite element method (FEM) model created in COMSOL Multiphysics.

The fabrication process used custom cavity SOI (CSOI) substrates (IceMOS Technology Ltd., Belfast, IE) with vacuum cavities formed under the 2.5 μm thick Si device layer. Following CSOI manufacture, a 20 nm thick seed AlN layer was first sputtered on the CSOI substrate to achieve a good crystalline structure of the subsequent Mo and AlN layers. Then a 200 nm Mo layer was sputtered as the bottom electrode in another chamber in the same system without breaking vacuum. A 1 μm AlN piezoelectric layer was then sputtered on the Mo bottom electrode layer. Following AlN deposition, vias were opened to contact the Mo bottom electrode with a reactive ion etching (RIE) process utilizing a combination of Cl_2 and BCl_3 gases with He used as diluent to improve etch uniformity. Finally, a 200 nm Al layer was evaporated and patterned by a lift-off process to form the top electrode and contact for the bottom electrode. Fig. 2 (a) and (b) show the optical image of the coupled PMUT along with an image of a 2x2 array of conventional PMUTs which occupies the same area. The fill-factor of the conventional array is 44%, while coupled designs 1 and 2 achieved 51% and 53% fill-factors. Fig. 2 (c) shows the cross section scanning electron microscope (SEM) image of the coupled PMUT membrane structure, CSOI cavities, and thin film layers.

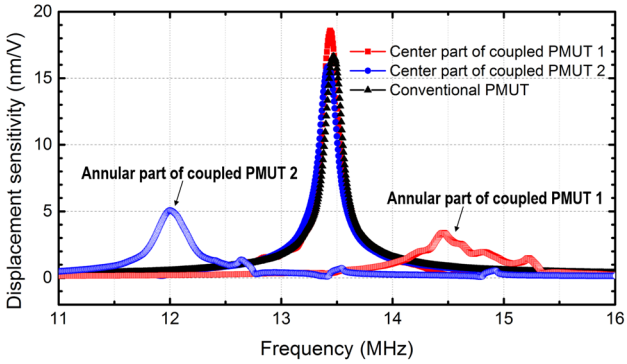

Fig. 3. LDV frequency response measurement in air.

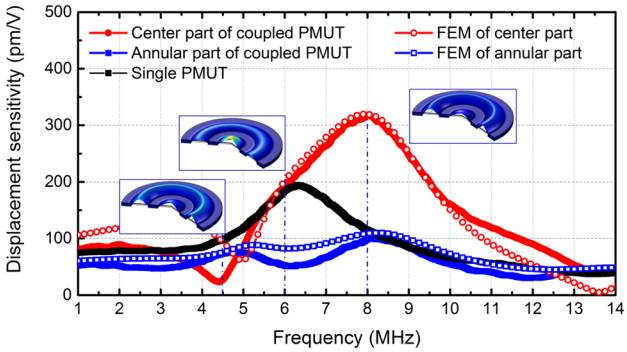

(a)

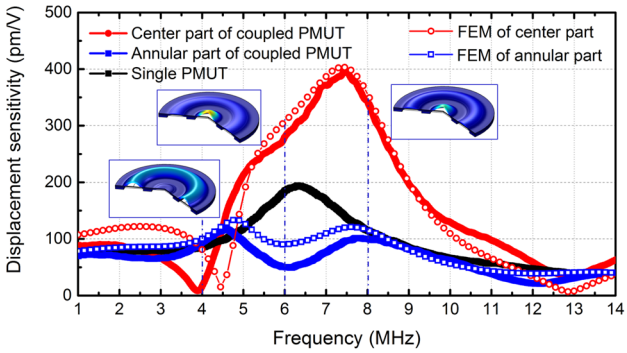

(b)

Fig. 4. Frequency response of immersed PMUTs: (a) coupled PMUT 1 and (b) coupled PMUT 2 compared to a conventional PMUT. Filled markers: measured LDV data; open markers: FEM models. The FEM simulated mode-shapes of the coupled PMUT occur at the frequencies indicated by the blue vertical dash-dot lines.

DYNAMIC RESPONSE

Fig. 3 shows the frequency response of a conventional PMUT and the two coupled PMUT designs measured via laser Doppler vibrometer (LDV) in conjunction with a network analyzer (E5061B, Agilent Technology) in air. The center membrane of the coupled designs has the same 13.5 MHz resonant frequency and displacement amplitude of 18 nm/V as the conventional PMUT due to the weak coupling in air. The resonant frequencies of the two annular membranes were 14.4 MHz for coupled PMUT 1 and 12.0 MHz for coupled PMUT 2 which are above and below the center membrane's resonance, as designed and in good agreement with the analytical model. Although the coupling in air is weak, small peaks can be observed in the response of the annular membranes at the resonant frequency of the center circular membrane.

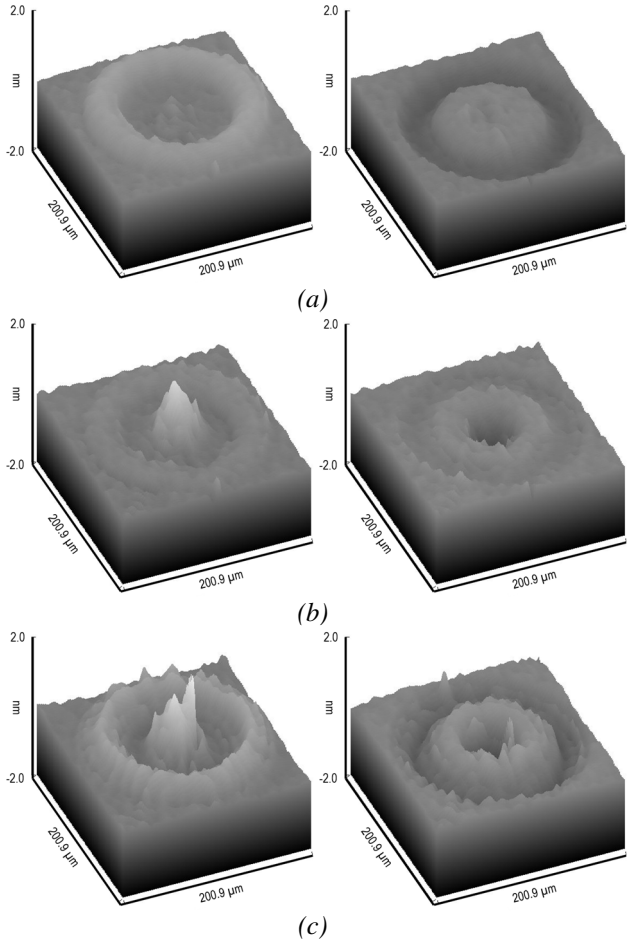

Fig. 5. DHM images of coupled PMUT 2 excited at (a) 4 MHz (b) 6 MHz and (c) 8 MHz. The images on the left correspond to the peak positive vibration and the images on the right correspond to the peak negative vibration.

Fig. 4 shows the frequency response of the three kinds of PMUTs immersed in Fluorinert. The filled markers represent experimental data which matches very well with the FEM simulation results shown with open markers. The three inset mode shapes in each figure were obtained with FEM simulation and illustrate: (1) the null around 4.5 MHz corresponds to the ring resonance; (2) the first peak near 6 MHz is the center membrane's resonance; (3) the maximum amplitude near 8 MHz is a coupled resonance mode between the center membrane and the annular membranes. Fig. 5 shows digital holographic microscope (DHM R1000, Lyncée Tec SA, Lausanne, CH) images of coupled PMUT 2 when driven under 4 MHz, 6 MHz and 8 MHz with 10 V_{pp}. Fig. 5 (a) shows the mode shape of coupled PMUT at 4 MHz where the center membrane has a minimum displacement amplitude and only the annular membrane is vibrating due to the coupling between the center and annular membranes. Fig 5 (b) shows that at 6 MHz, the center membrane vibration dominates. Fig. 5 (c) shows that at 8 MHz, both the center circular and annular membranes vibrate in-phase together with large amplitude thus generating a much larger total volume velocity. The measured DHM mode shapes are consistent with the results obtained via FEM shown in Fig. 4 (b).

The displacement amplitude at the center of the two coupled PMUT designs are 1.6 times and 2 times greater

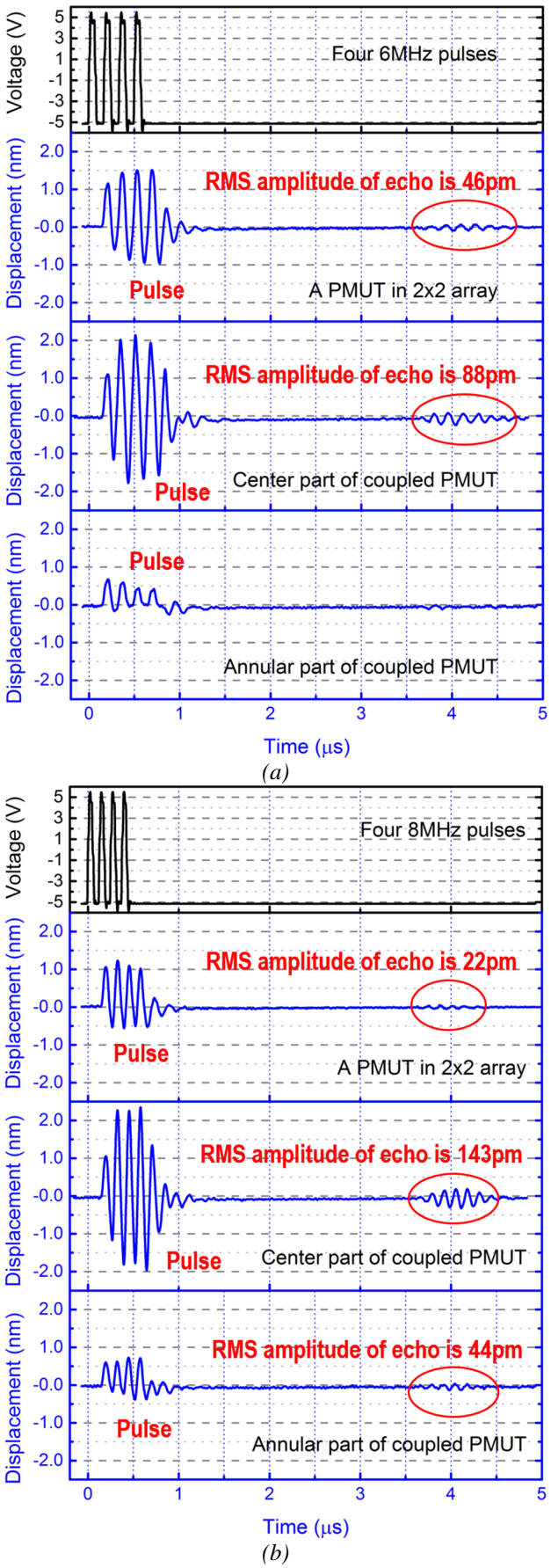

Fig. 6. Pulse-echo measurement at (a) 6 MHz and (b) 8 MHz for a PMUT in the 2x2 array and the center and annular part of coupled PMUT 2.

than that of the conventional circular PMUT due to coupling between the center membrane and the annulus through the fluid medium. The output pressure is proportional to the velocity at the PMUT surface, which can be computed by multiplying the displacement by the frequency, $2\pi f$. The velocity measured in the center of a circular PMUT (u_c) can be converted into volume velocity using $v_v = Au_c/3$, where A is the surface area of the PMUT. Consider the fundamental mode-shape of the annular membrane [7],

$$\phi(r) = \left[1 - \left(\frac{r-a}{b}\right)^2\right]^2 \quad (3)$$

where a is the inside radius and b is the outside radius of the annular membrane. The volume velocity, v_v, is

$$v_v = 2\pi \int_a^b r\phi(r)u_c\, dr \quad (4)$$

where u_c is the single-point velocity at the center of the annular membrane. When normalized to the array area, the calculated volume velocity of coupled PMUTs 1 and 2 is 1.2 times and 1.3 times greater than that of the 2x2 array, indicating a proportionate increase in transmit efficiency.

PULSE-ECHO RESPONSE

The immersed dynamic displacement of a conventional circular PMUT in a 2x2 array and of a coupled PMUT 2 was measured when both were driven with four 10 V_{pp} pulses at 6 MHz and 8 MHz. Fig. 6 (a) shows the dynamic responses under 6 MHz pulses. The transmit (TX) pulse's amplitude of coupled PMUT 2's center membrane was 1.94 nm RMS, 1.6 times larger than that of a PMUT in the 2x2 array, 1.2 nm RMS. This result is consistent with the frequency response as shown in Fig. 4 (b). The returning echo produced a 88 pm RMS receive (RX) signal at the center membrane of coupled PMUT 2 which is 1.9 times greater than the 46 pm RMS RX amplitude observed at the center of a PMUT in 2x2 array. The echo's time-of-arrival, 3.5 µs, corresponds to a round-trip distance of 2.6 mm which is consistent with the fluid height of ~1.3 mm. No clear RX echo is observed at the annular membrane of coupled PMUT 2, possibly due to the pressure distribution.

Fig. 6 (b) shows the TX-RX responses at 8 MHz. The TX displacement amplitude of the center of the coupled PMUT is ~ 2 nm RMS, 2.7 times higher than that of a PMUT in the 2x2 array, 0.75 nm RMS. The TX displacement amplitude of the annular membrane is ~ 1 nm RMS. The amplitude of the RX echo for a PMUT in the array is only 22 pm RMS, while it is 143 pm RMS and 44 pm RMS measured at the center and annular ring of the coupled PMUT. Comparing the coupled PMUT's peak RX response at 8 MHz, 143 pm RMS, to that of the conventional PMUT at its 6 MHz peak, 46 pm RMS, the coupled PMUT's RX response is a factor of 3.1x greater than the conventional design. The open-circuit RX voltage predicted using FEM for these displacement amplitudes are 2.8 mV and 0.7 mV, showing that the coupled PMUT's TX-RX pulse-echo response is a factor of 4 greater than that of the conventional design.

CONCLUSION

This paper presented a novel PMUT structure utilizing coupled energy between a center circular membrane and an outer annular membrane. The coupled design achieved a 7x increase in the pulse-echo performance compared to a conventional PMUT array with same area. The coupled PMUT had higher TX sensitivity, higher fill factor and higher output pressure. More importantly, the combination of the center and annular membranes offers new design space for large PMUT arrays with a unit cell of the same size as the acoustic wavelength for high array efficiency.

ACKNOWLEDGEMENTS

The authors thank UC Berkeley Marvelg Nanolab staff for help with the fabrication process, Berkeley Sensor and Actuator Center (BSAC) industrial members for financial support, IceMOS Technology for providing cavity SOI wafers and Lyncée Tec for the DHM measurements.

REFERENCES

[1] R. J. Przybyla, H. Y. Tang, S. E. Shelton, D. A. Horsley, and B. E. Boser, "12.1 3D ultrasonic gesture recognition," in *2014 IEEE International Solid-State Circuits Conference Digest of Technical Papers (ISSCC)*, 2014, pp. 210–211.

[2] Y. Lu, H. Tang, S. Fung, Q. Wang, J. M. Tsai, M. Daneman, B. E. Boser, D. A. Horsley, "Ultrasonic fingerprint sensor using a piezoelectric micromachined ultrasonic transducer array integrated with complementary metal oxide semiconductor electronics," *Appl. Phys. Lett.*, vol. 106, no. 26, p. 263503, Jun. 2015.

[3] A. Caronti, G. Caliano, R. Carotenuto, A. Savoia, M. Pappalardo, E. Cianci, V. Foglietti, "Capacitive micromachined ultrasonic transducer (CMUT) arrays for medical imaging," *Microelectron. J.*, vol. 37, no. 8, pp. 770–777, Aug. 2006.

[4] B. Belgacem, F. Calame, and P. Muralt, "Design, modeling and fabrication of piezoelectric micromachined ultrasonic transducers," in *2005 IEEE Ultrasonics Symposium*, 2005, vol. 1, pp. 483–486.

[5] Q. Wang, Y. Lu, S. Fung, X. Jiang, S. Mishin, Y. Oshmyansky, D. A. Horsley, "Scandium doped aluminum nitride based piezoelectric micromachined ultrasound transducers," in *Proc. of Solid-State Sensors, Actuators and Microsystems Work Shop*, Hilton Head, South Carolina, 2016, pp. 436–439.

[6] Y. Lu, H. Tang, Q. Wang, S. Fung, J. M. Tsai, M. Daneman, B. E. Boser, D. A. Horsley, "Waveguide piezoelectric micromachined ultrasonic transducer array for short-range pulse-echo imaging," *Appl. Phys. Lett.*, vol. 106, no. 19, p. 193506, May 2015.

[7] B. E. Eovino, S. Akhbari, and L. Lin, "Ring shaped piezoelectric micromachined ultrasonic transducers (PMUT) with increased pressure generation," in *Proc. of Hilton Head 2016*, 2016, pp. 432–445.

[8] R. D. Blevins, *Formulas for Natural Frequency and Mode Shape*. Krieger Publishing Company, 2001.

CONTACT

*Q. Wang, tel: +1-530-746-1632; qixwang@ucdavis.edu